

# Pulse-duration dependence of the double-to-single ionization ratio of Ne by intense 780-nm and 800-nm laser fields: Comparison of simulations with experiments

Zhangjin Chen, Lina Zhang, and Yali Wang

*Department of Physics, College of Science, Shantou University, Shantou, Guangdong 515063, People's Republic of China*

Oleg Zatsarinny and Klaus Bartschat

*Department of Physics and Astronomy, Drake University, Des Moines, Iowa 50311, USA*

Toru Morishita

*Institute for Advanced Science, The University of Electro-Communications, 1-5-1 Chofu-ga-oka, Chofu-shi, Tokyo 182-8585, Japan*

C. D. Lin

*J. R. Macdonald Laboratory, Physics Department, Kansas State University, Manhattan, Kansas 66506-2604, USA*



(Received 10 January 2019; revised manuscript received 14 March 2019; published 8 April 2019)

Accurate *ab initio* calculations of the ratio of double-to-single ionization of Ne atoms in strong laser fields are difficult due to the many-electron nature of the target. Here, with accurate total cross sections carefully evaluated by using the state-of-the-art many-electron *R*-matrix theory for both electron-impact ionization and electron-impact excitation of  $\text{Ne}^+$ , we simulate the total double-ionization yields of  $\text{Ne}^{2+}$  in strong laser fields at 780 and 800 nm for pulse durations in the range from 7.5 to 200 fs based on the improved quantitative rescattering model. The corresponding single-ionization yields of  $\text{Ne}^+$  are calculated within the nonadiabatic tunneling model of Perelomov, Popov, and Terent'ev. The ratio of double-to-single ionization of Ne is then obtained from the calculated double- and single-ionization yields. By normalizing the ratio to the one calculated from solving the time-dependent Schrödinger equation for a short few-cycle pulse, we make quantitative comparisons of our results with experimental data to show that our model predicts the experimental findings very well. Finally, we analyze the pulse-duration dependence of the double-to-single ionization ratio.

DOI: [10.1103/PhysRevA.99.043408](https://doi.org/10.1103/PhysRevA.99.043408)

## I. INTRODUCTION

Nonsequential double-ionization (NSDI) is the simplest and most fundamental correlated strong-field phenomenon. It has been extensively studied both experimentally and theoretically for more than three decades (for a review, see, e.g., Ref. [1]). The first evidence that strong-field NSDI occurs in favor of the classical recollision model [2,3] was provided by the very early experimental measurements of the total yield of doubly charged ions as a function of laser intensity [4–7], in which a characteristic knee structure was observed. The observed knee structure has certainly captured the attention of theorists. Several approaches, such as the quasistatic model [3], a simplified two-electron model including the effect of the outer electron on the inner one through a time-dependent potential [8], the *S*-matrix theory [9,10], and the classical ensemble model [11], have been employed. Although all the above theoretical simulations successfully reproduced the knee structure, quantitative comparison with experimental findings showed some discrepancies, especially for Ne atoms in strong laser fields with a wavelength of 780 nm [10]. While double-ionization yields versus laser intensity can be measured, it is preferable to study the ratios of double-to-single ionization yields. These ratios are more accurately determined in experiments and hence provide a more stringent test of the theoretical models.

Among all the rare-gas atoms, Ne is the one for which the simulated double-to-single ionization ratios deviate most from experiment. It was reported two decades ago that a sensitive measure of the intensity dependence of the double-to-single ionization ratio of Ne in a strong 780-nm laser field decreases by approximately a factor of 10 below the saturation intensity where the absolute ratio is about  $1.8 \times 10^{-3}$ , which is very similar to the measurement for He [12]. Interestingly, the early simulated results by the semiclassical model were significantly different for Ne and He, and they substantially underestimated the experimental values for both Ne and He [12]. By now, the measured intensity dependence of the double-to-single ionization ratio of He in 780-nm laser pulses [12] has already been remarkably well reproduced by several theoretical models [10,13–15]. On the contrary, the  $\text{Ne}^{2+}/\text{Ne}^+$  ratio measured in the same range of intensity at the same wavelength has only been simulated by the *S*-matrix theory, which overestimates the experimental data by a factor of 15 [10].

According to the classical recollision model, an electron that initially tunneled out from an atom could be driven back to the nucleus to collide with a bound electron and set it free in the combined atomic and electric-field potential. For long pulses, electrons that have been released earlier may return at different times. As a result, the total probability of double

ionization depends on the number of returns and therefore on the number of optical cycles in the laser pulse. The pulse-duration dependence of the double-to-single ionization ratio was studied by Bhardwaj *et al.* [16] by measuring the ratio of  $\text{Ne}^{2+}/\text{Ne}^+$  yields as a function of peak intensity in 50 and 12 fs pulses with the wavelength of 800 nm. Bhardwaj *et al.* also performed numerical simulations by using a semiclassical model based on the rescattering mechanism. However, quantitative comparisons with the experimental data were not available, since the calculations were only performed for He due to the lack of sufficient theoretical and experimental data of total cross sections (TCSs) for electron-impact ionization and electron-impact excitation of  $\text{Ne}^+$  ion at that time.

Recently, we calculated the TCSs for electron-impact ionization and electron-impact excitation of  $\text{Ne}^+$  ion using the state-of-the-art many-electron  $R$ -matrix (close-coupling) theory. With these carefully evaluated TCSs, we were able to simulate the ratio of  $\text{Ne}^{2+}/\text{Ne}^+$  yields as a function of peak intensity in a 40 fs pulse with a wavelength of 400 nm. Indeed, the calculated results are in very good agreement with experiment [17].

In the present paper, the ratio between double and single ionization of Ne by intense laser pulses at wavelengths of 780 and 800 nm with different pulse durations in the range from 7.5 fs to 200 fs are simulated. We aim to make quantitative comparisons of our model results with the experimental data. Special attention is also paid to the pulse-duration dependence of the ratio between double and single ionization. Unless specified otherwise, atomic units are used throughout this paper.

## II. THEORETICAL MODEL

The theoretical model used in this paper to simulate the double-to-single ionization ratio for atoms in linearly polarized laser pulses was presented in detail in Refs. [15,17]. Hence we only give a brief review here.

To obtain the ratio of double-to-single ionization as a function of laser intensity, both the double- and single-ionization yields need to be evaluated. The total single-ionization yield can be obtained reliably by using the standard strong-field approximation [18,19], which was also referred to as SFA1 [20]. Alternatively, a simpler ionization model proposed by Perelomov, Popov, and Terent'ev (PPT) [21], which was improved later by Popruzhenko *et al.* [22], is often preferred. Recently, the improved PPT model was used to calibrate the laser intensity in strong-field ionization experiments [23]. It was also demonstrated that the PPT model is fully capable of reproducing single-ionization probabilities for atoms in laser fields from the multiphoton to the tunneling-ionization regimes [24]. While the SFA1 model was used in Refs. [15,17], in the present paper we employ the improved PPT model to calculate the single-ionization yield for Ne atoms.

To calculate the total nonsequential double-ionization yields, we employ the improved quantitative rescattering (QRS) model [15,17], in which the lowering of the required energy for electrons to escape from the nucleus at the time of recollision, due to the presence of an electric field, is taken into account. The QRS model was first proposed for high-order above-threshold ionization (HATI) attributed to

elastic scattering of the returning electron from the parent ion [25]. The past decade has witnessed great success of the QRS model in dealing with various laser-induced rescattering processes [26,27].

According to the QRS model [25], the momentum distribution of the HATI photoelectron with momentum  $\mathbf{p}$  can be factorized as the product of a returning electron wave packet (RWP) and the elastic electron differential scattering cross section (DCS),

$$D(\mathbf{p}) = W(k_r) \frac{d\sigma(k_r, \theta_r)}{d\Omega_r}, \quad (1)$$

where  $d\sigma(k_r, \theta_r)/d\Omega_r$  is the DCS for an electron with a momentum of magnitude  $k_r$  to be scattered at an angle  $\theta_r$  with respect to the direction of the returning electron, and  $W(k_r)$  is the RWP describing the momentum distribution of the returning electrons. The detected photoelectron momentum  $\mathbf{p}$  and the momentum  $\mathbf{k}_r$  of the scattered electron are related by

$$\mathbf{p} = \mathbf{k}_r - \mathbf{A}_r, \quad (2)$$

with

$$k_r = 1.26|\mathbf{A}_r|, \quad (3)$$

where  $\mathbf{A}_r$  is the instantaneous vector potential at the time of recollision.

Applying the QRS model to NSDI, the total ionization yield in a linearly polarized laser pulse with electric field along the  $z$  axis can be expressed by [17]

$$\mathcal{Y}^{2+} = \int dE_r [W_L(E_r) + W_R(E_r)] \times [\sigma_{\text{exc}}(E_r + 2\sqrt{|F_r|}) + \sigma_{e2e}(E_r + 2\sqrt{2|F_r|})], \quad (4)$$

where  $E_r = k_r^2/2$  is the energy of the returning (incident) electron,  $F_r$  is the electric field at the instant of recollision,  $\sigma_{\text{exc}}$  ( $\sigma_{e2e}$ ) is the TCS for laser-free electron impact excitation (ionization) of the parent ion, and  $W_L$  ( $W_R$ ) is the RWP for electrons returning to the parent ion along  $+\hat{z}$  ( $-\hat{z}$ ). Here we assume that all excited atomic ions will be ionized in the subsequent strong laser field. It should be noted that, similar to Eq. (4), factorization of the double-ionization yield was also suggested by Kuchiev [28], who proved that the two-electron amplitude may be presented as a product of the amplitude for single-electron ionization and the amplitude for electron-ion inelastic scattering in the presence of a laser field.

The RWP in Eq. (4) can be evaluated by using Eq. (1), in which the HATI photoelectron momentum distributions are calculated based on the second-order strong-field approximation (SFA2) [20,25] while the elastic scattering DCSs are calculated within the plane-wave first-order Born approximation (PWBA). It should be noted that, in the calculations of the RWP for NSDI of Ne in laser fields of long pulses and high intensities, the depletion of the ground state is taken into account in the SFA2 model. In our previous work [17], we used a hydrogen-like wave function to describe the ground state of Ne. Here, the ground-state wave function is obtained by an expansion in a Slater basis, where the radial part takes the form

$$R_{2p}(r) = \sum_i c_i \frac{1}{\sqrt{(2n_i)!}} (2\xi_i)^{n_i+1/2} r^{n_i-1} e^{-\xi_i r}. \quad (5)$$

The parameters  $c_i$ ,  $n_i$ , and  $\xi_i$  are given by Clementi and Roetti [29].

The TCSs for laser-free electron-impact excitation and electron-impact ionization of the  $\text{Ne}^+$  ion are calculated with the close-coupling with pseudostates method using the fully parallelized  $B$ -spline  $R$ -matrix code [30]. In such calculations the many-electron correlation effects are included at the “state-of-the-art” level typically used in laser-free electron-impact excitation and ionization cross-section calculations.

It should be emphasized that absolute values for both double- and single-ionization yields have to be obtained in order to simulate the double-to-single ionization ratio. Since the SFA2 model is unable to reproduce absolute RWPs, the simulated double-ionization yields using Eq. (4) do not give the correct absolute double-ionization yields. However, it has been demonstrated that, except for a normalization factor, the RWP from SFA2 exhibits the same momentum or energy dependence of the laser-induced returning electron as the RWP obtained from solving the time-dependent Schrödinger equation (TDSE) [25]. Since the RWP from the TDSE ( $W_{\text{TDSE}}$ ) is absolute, the absolute RWP ( $W_{\text{abs}}$ ) for a laser pulse at a peak intensity  $I$  with a wavelength  $\lambda$  and a pulse duration  $\Gamma$  can be obtained by renormalizing the RWP from SFA2 ( $W_{\text{SFA2}}$ ) [17] according to

$$W_{\text{abs}}(I, \lambda, \Gamma) = C(I, \lambda, \Gamma)W_{\text{SFA2}}(I, \lambda, \Gamma), \quad (6)$$

where the normalization factor is given by

$$C(I, \lambda, \Gamma) = \frac{W_{\text{TDSE}}(I, \lambda, \Gamma)}{W_{\text{SFA2}}(I, \lambda, \Gamma)}. \quad (7)$$

Nevertheless, the above equations only mean that  $W_{\text{abs}}(I, \lambda, \Gamma) = W_{\text{TDSE}}(I, \lambda, \Gamma)$ . However, as will be demonstrated in the next section, the normalization factor is almost independent of the pulse duration. Consequently, Eq. (7) can be approximately rewritten as

$$C(I, \lambda, \Gamma) \simeq C(I, \lambda, \Gamma') = \frac{W_{\text{TDSE}}(I, \lambda, \Gamma')}{W_{\text{SFA2}}(I, \lambda, \Gamma')}. \quad (8)$$

Since RWP calculations by solving TDSE can hardly be performed for long pulses at high intensities, we chose a few-cycle short pulse with  $\Gamma' = 5$  fs in the actual calculations for the normalization factor. For single ionization, we applied a similar procedure using the ionization probability from solving the TDSE for a short pulse at low intensity to renormalize the ionization probability from the PPT theory. Details of the TDSE calculations and the normalization procedure can be found in Refs. [31] and [17], respectively.

### III. RESULTS AND DISCUSSION

To evaluate the total NSDI yield for Ne at a single peak intensity using Eq. (4), we need to prepare the TCSs for electron-impact ionization and electron-impact excitation of  $\text{Ne}^+$  as well as the RWPs of the returning electrons. By single peak intensity, we mean that no focal volume integral is performed in the calculations. Figure 1 displays the TCSs calculated with the  $R$ -matrix method. For electron-impact excitation of  $\text{Ne}^+$ , the TCSs for excitations to the 12 excited states from  $2s2p^6$  to  $2s^22p^45f$  are evaluated explicitly. Excitations to higher excited states are neglected based on the  $n^{-3}$  scaling

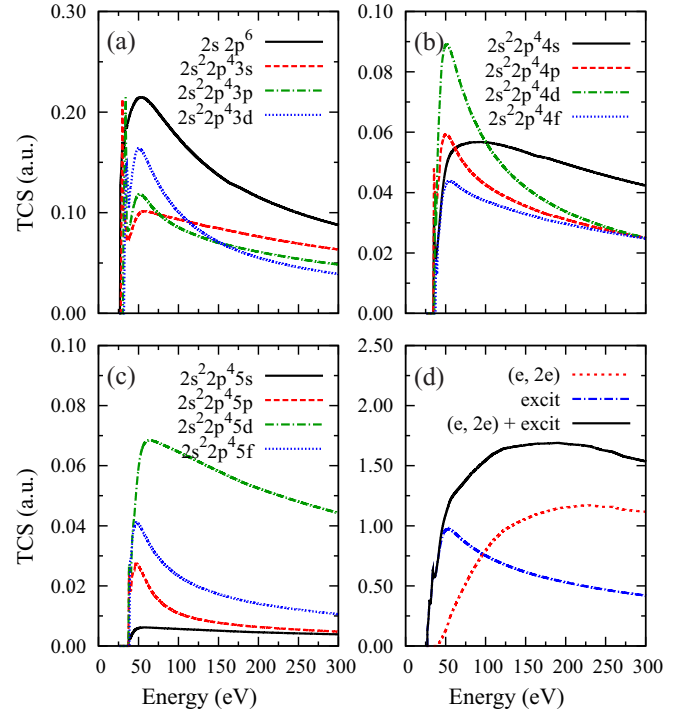


FIG. 1. Total cross sections for electron-impact ionization and excitation of  $\text{Ne}^+$  from the ground state. Excitation of the configurations (a)  $2s2p^6$ ,  $2s^22p^43s$ ,  $2s^22p^43p$ , and  $2s^22p^43d$ ; (b)  $2s^22p^44s$ ,  $2s^22p^44p$ ,  $2s^22p^44d$ , and  $2s^22p^44f$ ; (c)  $2s^22p^45s$ ,  $2s^22p^45p$ ,  $2s^22p^45d$ , and  $2s^22p^45f$ . Panel (d) shows the summed total cross sections for ionization and excitation of all configurations in panels (a)–(c).

law. As demonstrated in Figs. 1(a)–1(c), the present numerical calculations are consistent with the well-known energy dependence that the TCSs for each excited state first grows with the incident electron energy from the threshold to a peak, which is then followed by a smooth decrease as the electron energy is further increased. Sharp narrow resonances lying close to the threshold energies for some low-lying excited states are also predicted. From the calculated results, it is interesting to see that the TCSs for excitation to the lowest excited state  $2s2p^6$  are substantially larger than those for all other excited states. This is in contrast to the case of  $\text{Ar}^+$ , in which excitation to  $3s^23p^43d$  is dominant owing to the large overlap of the  $3d$  orbital with the  $3p$  orbital [32]. The sum of the TCSs for excitations to the 12 excited states from  $2s2p^6$  to  $2s^22p^45f$  is shown in Fig. 1(d); it exhibits a similar energy dependence as those for each individual excited state. On the other hand, it can be seen from Fig. 1(d) that the energy dependence of the TCSs for ionization is substantially different from that for excitation. Close to threshold, the ionization cross sections increase slowly with increasing incident energy, becoming comparable to the excitation cross sections around 100 eV before reaching a maximum just below 230 eV. The energy dependence of the TCSs for excitation and ionization shown in Fig. 1(d) indicates that excitation dominates NSDI in Ne for laser intensities below  $5.2 \times 10^{14}$  W/cm<sup>2</sup>, corresponding to the highest returning electron energy of approximately 100 eV. For higher intensities, on the other hand, the relative

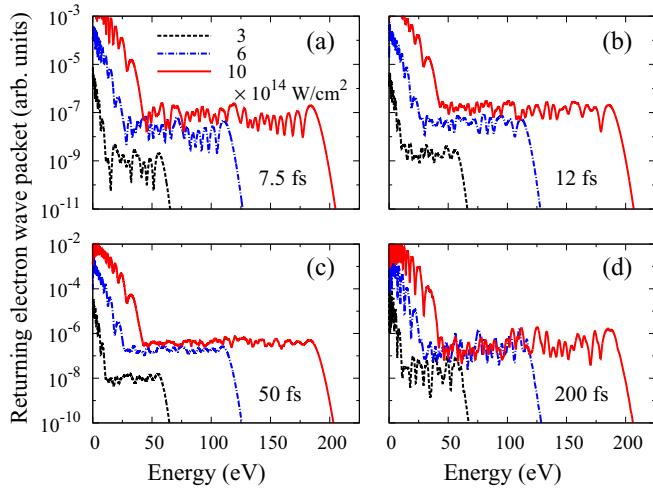


FIG. 2. Returning electron wave packets  $W_R(E_r)$  for Ne in linearly polarized 800-nm laser fields with pulse durations of (a) 7.5 fs, (b) 12 fs, (c) 50 fs, and (d) 200 fs at single peak intensities of 3, 6, and  $10 \times 10^{14}$  W/cm<sup>2</sup>, respectively. The sharp rapid oscillations in the returning electron wave packets were smoothed out to improve the visibility.

contributions from excitation decrease with respect to the contributions from ionization.

It is well recognized [32,33] that laser-induced excitation affects the NSDI yield and could be a primary route to NSDI, especially at low laser intensities, since excitation cross sections are typically larger than the ionization cross sections [34]. Of course, in the meanwhile, ionization cross sections alone have also been shown [35] to give significant insight into NSDI. Previously, in the simulations for total ionization yields of doubly charged ions, the Lotz formula [36] as well as other empirical formulas [37] were widely used to evaluate the TCSs for electron-impact ionization and electron-impact excitation of ions [10,38–40]. From a purely theoretical point of view, empirical formulas (even if they work well for some cases) are certainly inferior, irrespective of their convenience. Therefore, accurate cross sections for both electron-impact ionization and electron-impact excitation of ions, such as the TCSs obtained with the *R*-matrix method shown in Fig. 1, are highly desirable.

Figure 2 displays the RWPs for Ne in a linearly polarized 800-nm laser field with pulse durations of 7.5, 12, 50, and 200 fs at the individual peak intensities of 3, 6, and  $10 \times 10^{14}$  W/cm<sup>2</sup>, respectively. From Eq. (4), one can see that the RWPs  $W_R(E_r)$  and  $W_L(E_r)$  actually indicate the weight of the contribution to the total yield of doubly charged ion at incident energy  $E_r$ . For laser pulses longer than 12 fs,  $W_R(E_r) = W_L(E_r)$ . As expected, each RWP starts with a fast drop at low energies before becoming flat in the plateau region with a cutoff at  $3.17 U_p$ , where  $U_p$  is the ponderomotive energy. Nevertheless, while the plateau of the RWP at the intensity of  $10 \times 10^{14}$  W/cm<sup>2</sup> is about five times higher than that at  $6 \times 10^{14}$  W/cm<sup>2</sup> for the pulse durations of 7.5 and 12 fs, the difference in height of the plateau between the two intensities becomes smaller for longer pulses. For the 200 fs laser pulse, the RWPs at 6 and  $10 \times 10^{14}$  W/cm<sup>2</sup> lie almost on top of each other in the plateau region. This is due to the

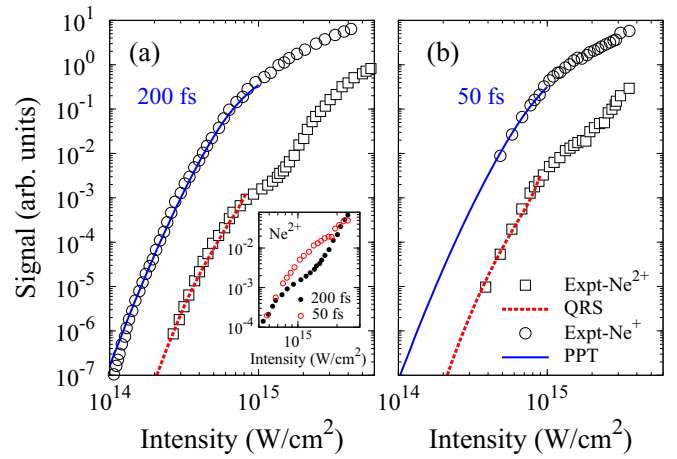


FIG. 3. Double- and single-ionization yields for Ne exposed to linearly polarized laser pulses at 800 nm with pulse durations of (a) 200 fs and (b) 50 fs. The experimental data shown in panels (a) and (b) are taken from Larochelle *et al.* [41] and Bhardwaj *et al.* [16], respectively. The simulated results from the QRS model for double ionization and the PPT model for single ionization are normalized for good visual agreement with experiment. The calculations include the integration over the focal volume of the laser. The inset shows the measured knee structure in the double-ionization yield for 200 and 50 fs pulses, respectively.

ionization yield becoming saturated at high laser intensities before the pulse is over for long pulses.

With the calculated RWP at each intensity and the precalculated TCSs for both excitation and ionization, the total yield of doubly charged ion for NSDI at each individual intensity can be evaluated by using Eq. (4). Furthermore, by taking into account focal volume averaging, the obtained total yield for doubly charged ions as a function of the experimental peak laser intensity can be compared directly with the experimental data. In Fig. 3, we compare the simulated double- and single-ionization yields with the experimental measurements for Ne exposed to linearly polarized laser pulses at 800 nm with pulse durations of 200 fs [41] and 50 fs [16], respectively. The experimental and the theoretical results agree remarkably well for the intensity range considered here. In the inset of Fig. 3, one also observes that the characteristic knee structure measured in the experiment for 200 fs appears at lower intensity than it does for 50 fs. As explained before, this is due to the saturation onset occurring at a lower intensity for longer pulses [31].

As mentioned in the previous section, to simulate the double-to-single ionization ratio, one needs to obtain the absolute values for both double- and single-ionization yields. The absolute values for double-ionization yields can be obtained by calibrating the RWP from SFA2 by using Eq. (8). Since TDSE calculations are extremely formidable for long laser pulses at high intensities, we only evaluated the RWP by solving the TDSE for Ne in a linearly polarized 800-nm laser field with pulse durations of 5 and 10 fs at single peak intensities of 1.8, 2.5, and  $3.6 \times 10^{14}$  W/cm<sup>2</sup>. In Figs. 4(a)–4(c) some of the calculated RWPs of TDSE are compared with the corresponding RWPs of SFA2 with normalization factors. With these normalization factors, the RWPs of SFA2

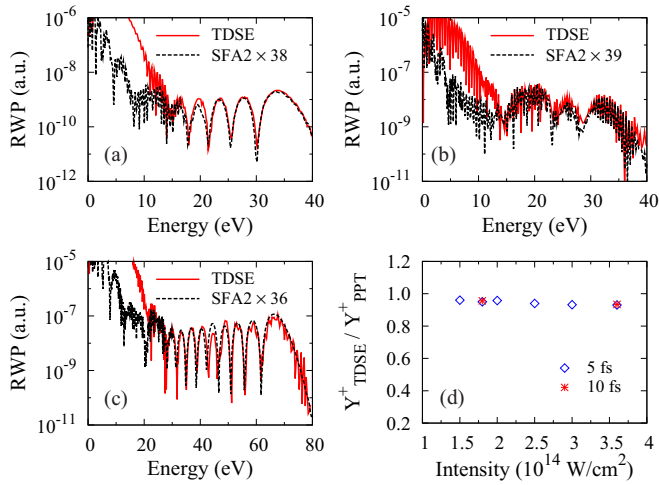


FIG. 4. Comparison of the returning electron wave packets from TDSE and SFA2 for Ne in a linearly polarized 800-nm laser field with parameters of (a) 5 fs and  $1.8 \times 10^{14}$  W/cm<sup>2</sup>, (b) 10 fs and  $1.8 \times 10^{14}$  W/cm<sup>2</sup>, and (c) 5 fs and  $3.6 \times 10^{14}$  W/cm<sup>2</sup>. Panel (d) shows the ratio of the single-ionization yield from TDSE ( $Y_{\text{TDSE}}^+$ ) over the single-ionization yield of PPT ( $Y_{\text{PPT}}^+$ ) for Ne in a linearly polarized 800-nm laser field as a function of intensity for pulse durations of 5 and 10 fs, respectively. In panels (a)–(c), the returning electron wave packets of SFA2 are renormalized according to the corresponding TDSE results.

are in very good agreement with those of TDSE at the plateau region. This clearly indicates that the RWP of TDSE can be well reproduced by the SFA2 model with an appropriate rescaling factor. In addition, it is demonstrated that the normalization factors for different laser pulses and different laser intensities are quite close. Consequently, one can deduce that the normalization factor does not depend on the pulse duration or the laser intensity. It should be noted that the RWPs of TDSE are extracted from the two-dimensional momentum distributions. Since the contributions from direct ionization and laser-induced rescattering cannot be separated in the HATI spectra of TDSE at energies below  $4U_p$ , the RWP of TDSE in the low-energy region, where the RWP decreases rapidly, includes impurity from direct ionization. This impurity makes it much larger than the RWP of SFA2 where direct ionization is excluded. Similarly, one can also use the TDSE results to calibrate the total ionization yields from the PPT theory. In Fig. 4(d) we show the ratio of the single-ionization yield from TDSE over the single-ionization yield of PPT for Ne in a linearly polarized 800-nm laser field as a function of intensity for pulse durations of 5 and 10 fs, respectively. It is interesting to see that the ratios of  $Y_{\text{TDSE}}^+ / Y_{\text{PPT}}^+$  at different intensities are almost constant and very close to 1. This indicates that the PPT theory is a good candidate to evaluate the total single-ionization yield, and the ratio of  $Y_{\text{TDSE}}^+ / Y_{\text{PPT}}^+$  does not depend on the pulse duration and the laser intensity, either. We should emphasize that this pulse-length-independent normalization is valid only at intensities when ionization saturation has not occurred yet and for pulses that are not too short such that a carrier-envelope-phase (CEP) dependence is significant.

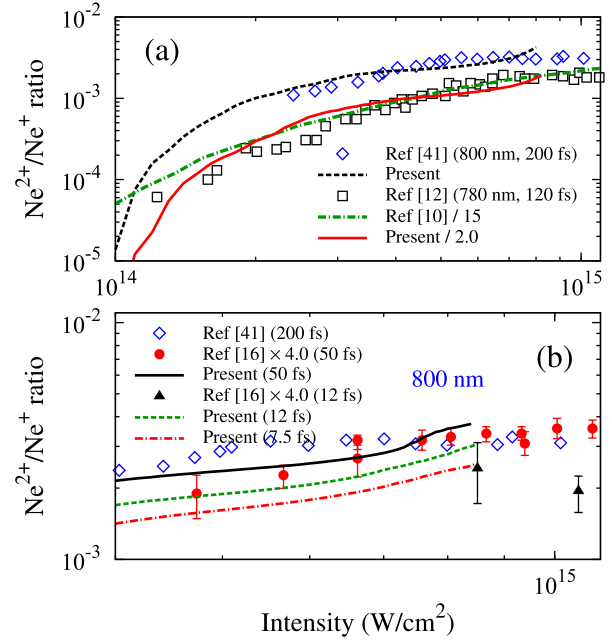


FIG. 5. Ratio between double and single ionization as a function of intensity for Ne exposed to linearly polarized laser pulses with (a) pulse duration of 200 fs at a wavelength of 800 nm and pulse duration of 120 fs at a wavelength of 780 nm, and (b) pulse durations of 7.5, 12, 50, and 200 fs at a wavelength of 800 nm. In panel (a), the present simulations are compared with the experimental data of Larochelle *et al.* [41] and Sheehy *et al.* [12], as well as with the  $S$ -matrix calculations of Becker and Faisal [10]. In panel (b), the present results are compared with the experimental data of Bhardwaj *et al.* [16]. See text for details.

Once the total ionization yields for both double and single ionizations are renormalized, one is ready to obtain the double-to-single ionization ratio. In Fig. 5(a), the present simulated double-to-single ionization ratios for Ne exposed to a linearly polarized 200 fs laser pulse at a wavelength of 800 nm and by a 120 fs pulse at a wavelength of 780 nm are compared with the experimental data. For the 200 fs 800-nm pulse, the experimental double-to-single ionization ratios are deduced from the measured total ionization yields of  $\text{Ne}^{2+}$  and  $\text{Ne}^+$  by Larochelle *et al.* [41]. The simulations agree very well for intensities up to  $8.0 \times 10^{14}$  W/cm<sup>2</sup>. For the 120 fs 780-nm pulse, an earlier calculation was reported by Becker and Faisal using the  $S$ -matrix theory [10]. Comparing our present results and theirs with the experiments reported in Sheehy *et al.* [12], the two calculations for the ratios are about 2 and 15 times higher than the experimental data. Since the wavelengths used in the two experiments are quite close and the pulse durations are multiple cycles, we would expect the double-to-single ionization ratios in the two experiments to also be close to each other. Given that we have good agreement with the data of Larochelle *et al.* [41], we suggest that the data of Sheehy *et al.* [12] were underestimated. The larger discrepancy from Becker and Faisal [10] is not unexpected, since they used a much simpler model and many-electron correlation effects were not included in their theory.

In Fig. 5(b), we compare the present model calculations with the experimental data of the double-to-single ionization

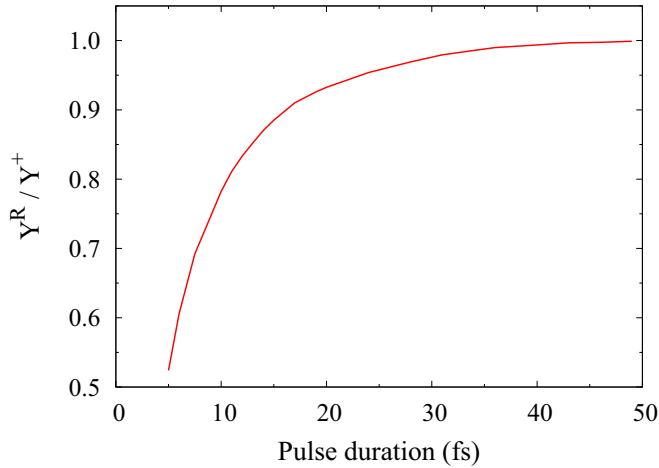


FIG. 6. Pulse-duration dependence of the ratio between the total yield of returning electrons  $Y^R$  and the total yield of single ionization  $Y^+$  for Ne in an 800-nm pulse at a peak intensity of  $6.0 \times 10^{14} \text{ W/cm}^2$ . The ratio  $Y^R/Y^+$  is normalized to unity at 50 fs. See text for details.

ratio for Ne in laser pulses at 800 nm with pulse durations of 50 and 12 fs performed by Bhardwaj *et al.* [16]. The latter were multiplied by a factor of four such that the data for Ne in a 50 fs pulse are comparable to the measurements of Larochelle *et al.* [41] in a 200 fs pulse. After this renormalization, we note that our results for the 50 fs pulse are in good agreement with the data of Bhardwaj *et al.* [16]. For the 12 fs pulses, experimental data are not available for intensities below  $8 \times 10^{14} \text{ W/cm}^2$ . Above this intensity, the measured  $\text{Ne}^{2+}/\text{Ne}^+$  ratios with the 12 fs pulses are about 60% lower than those for the 50 fs pulses, after the same factor-of-four renormalization, thereby indicating a pulse-duration dependence of the ratio of double-to-single ionization for short pulses. Such pulse-duration dependence is seen in our theoretical simulations in Fig. 5(b) where the ratios were calculated for pulse durations of 50, 12, and 7.5 fs, respectively. Note that all the theoretical simulations and experimental data indicate that the double-to-single ionization ratios increase with laser intensities. This is not the case for the experimental data at the two intensity points for the 12 fs pulses shown Fig. 5(b).

As mentioned in Sec. I, Bhardwaj *et al.* [16] also performed theoretical simulations, using the semiclassical model [33] based on the rescattering mechanism, to predict the pulse-duration dependence of the double-to-single ionization ratio. In the semiclassical simulations, the probability for the recollision of the active electron with the parent ion, including not only ionization but also excitation to all states, is determined by the total inelastic cross section of this collision. However, in Ref. [16] calculations were only performed for He due to the lack of theoretical or experimental data for total inelastic cross sections for the  $\text{Ne}^+$  ion.

According to the QRS model used in our simulations, the pulse-duration dependence of double ionization related to the rescattering process is attributed mainly to the pulse-duration dependence of the RWP. In Fig. 6 we show the ratio of the total yield  $Y^R$  of the returning electrons to the total yield  $Y^+$  of

single ionization of Ne by 800-nm pulses, at a single peak intensity of  $6.0 \times 10^{14} \text{ W/cm}^2$ , as a function of pulse duration. The yield of returning electrons is obtained by integrating the RWP over the returning electron energies above the threshold. Since the RWP for short pulses depends on the CEP, the RWPs used here are CEP-averaged. One can see that the ratio  $Y^R/Y^+$  increases rapidly with increasing pulse duration until 15 fs, followed by a slower increase toward a constant for durations above 30 fs. Figure 6 clearly demonstrates that the ratio  $Y^R/Y^+$  reveals a very simple pulse-duration dependence, which mainly reflects the pulse-duration dependence of the double-to-single ionization ratio. According to the QRS model, the ratio  $Y^R/Y^+$  shown in Fig. 6 is expected to be independent of the target, but it depends only on the properties of the laser pulses used in experiment. We comment that other models in the literature interpret the pulse-duration dependence based on specific calculations. For example, Ho and Eberly [42] attribute the pulse-duration dependence to multiple recollisions or Coulomb focusing [43].

#### IV. CONCLUSIONS

We have simulated the double-to-single ionization ratio for Ne atoms exposed to a linearly polarized laser pulse at 780 nm with pulse duration of 120 fs and laser pulses at 800 nm with pulse durations of 7.5, 12, 50, and 200 fs. The simulated results are compared directly with available experimental data. For 780-nm and 120 fs laser pulses, the present QRS model predicts double-to-single ionization ratios that are higher by about a factor of two than the experimental data [12]. Nevertheless, the double-to-single ionization ratio deduced from the measured double- and single-ionization yields for Ne in an 800-nm 200 fs pulse [41] is well reproduced by our model calculations. The present simulations are also found to be in good agreement with the renormalized experimental data of Bhardwaj *et al.* [16] for the double-to-single ionization ratio of Ne in 800-nm pulses with pulse durations of 50 and 12 fs. The experimental data of Bhardwaj *et al.* [16] were renormalized such that the double-to-single ionization ratio in a 50 fs pulse is comparable to that for a 200 fs pulse. This is justified by the finding that a pulse-duration dependence is not expected above about 30 fs, as shown in Fig. 6. The present work indicates that, with accurate cross sections for electron-impact ionization and excitation of  $\text{Ne}^+$  available from our  $R$ -matrix calculations, the NSDI processes for Ne under an intense laser pulse can be readily simulated and the results be compared directly to experiments. The theoretical methods presented here can be extended to NDSI for Ne by other lasers, including multicolor laser pulses.

#### ACKNOWLEDGMENTS

This work was supported by the National Natural Science Foundation of China under Grant No. 11274219 and the Scientific Research Foundation for the Returned Overseas Chinese Scholars, State Education Ministry. O.Z. and K.B. were supported by the United States National Science Foundation under Grants No. PHY-1430245, No. PHY-1520970, and No. PHY-1803844, as well as by the XSEDE Allocation No. PHY-090031. T.M. was supported in part by the

Japan Society for the Promotion of Science KAKENHI Grants No. 16H04029, No. 16H04103, and No. 17K05597. C.D.L. was supported, in part, by the Chemical Sciences,

Geosciences and Biosciences Division, Office of Basic Energy Sciences, Office of Science, United States Department of Energy, under Grant No. DE-FG02-86ER13491.

- [1] W. Becker, X. Liu, P. Ho, and J. H. Eberly, *Rev. Mod. Phys.* **84**, 1011 (2012).
- [2] K. J. Schafer, Baorui Yang, L. F. DiMauro, and K. C. Kulander, *Phys. Rev. Lett.* **70**, 1599 (1993).
- [3] P. B. Corkum, *Phys. Rev. Lett.* **71**, 1994 (1993).
- [4] A. L'Huillier, L. A. Lompre, G. Mainfray, and C. Manus, *Phys. Rev. Lett.* **48**, 1814 (1982); *Phys. Rev. A* **27**, 2503 (1983).
- [5] D. N. Fittinghoff, P. R. Bolton, B. Chang, and K. C. Kulander, *Phys. Rev. Lett.* **69**, 2642 (1992).
- [6] B. Walker, E. Mevel, B. Yang, P. Breger, J. P. Chambaret, A. Antonetti, L. F. DiMauro, and P. Agostini, *Phys. Rev. A* **48**, R894 (1993).
- [7] B. Walker, B. Sheehy, L. F. DiMauro, P. Agostini, K. J. Schafer, and K. C. Kulander, *Phys. Rev. Lett.* **73**, 1227 (1994).
- [8] J. B. Watson, A. Sanpera, D. G. Lappas, P. L. Knight, and K. Burnett, *Phys. Rev. Lett.* **78**, 1884 (1997).
- [9] A. Becker and F. H. M. Faisal, *Phys. Rev. A* **59**, R1742 (1999).
- [10] A. Becker and F. H. M. Faisal, *J. Phys. B: At., Mol. Opt. Phys.* **32**, L335 (1999).
- [11] P. J. Ho, R. Panfili, S. L. Haan, and J. H. Eberly, *Phys. Rev. Lett.* **94**, 093002 (2005).
- [12] B. Sheehy, R. Lafon, M. Widmer, B. Walker, L. F. DiMauro, P. A. Agostini, and K. C. Kulander, *Phys. Rev. A* **58**, 3942 (1998).
- [13] H. W. van der Hart and K. Burnett, *Phys. Rev. A* **62**, 013407 (2000).
- [14] G. L. Yudin and M. Yu. Ivanov, *Phys. Rev. A* **64**, 035401 (2001).
- [15] Z. Chen, Y. Zheng, W. Yang, X. Song, J. Xu, L. F. DiMauro, O. Zatsarinny, K. Bartschat, T. Morishita, S.-F. Zhao, and C. D. Lin, *Phys. Rev. A* **92**, 063427 (2015).
- [16] V. R. Bhardwaj, S. A. Aseyev, M. Mehendale, G. L. Yudin, D. M. Villeneuve, D. M. Rayner, M. Yu. Ivanov, and P. B. Corkum, *Phys. Rev. Lett.* **86**, 3522 (2001).
- [17] Z. Chen, X. Li, O. Zatsarinny, K. Bartschat, and C. D. Lin, *Phys. Rev. A* **97**, 013425 (2018).
- [18] M. Lewenstein, K. C. Kulander, K. J. Schafer, and P. H. Bucksbaum, *Phys. Rev. A* **51**, 1495 (1995).
- [19] D. B. Milošević, A. Gazibegović-Busuladžić, and W. Becker, *Phys. Rev. A* **68**, 050702(R) (2003).
- [20] Z. Chen, T. Morishita, A.-T. Le, and C. D. Lin, *Phys. Rev. A* **76**, 043402 (2007).
- [21] A. M. Perelomov, V. S. Popov, and M. V. Terent'ev, *Sov. Phys. JETP* **24**, 207 (1967).
- [22] S. V. Popruzhenko, V. D. Mur, V. S. Popov, and D. Bauer, *Phys. Rev. Lett.* **101**, 193003 (2008).
- [23] S.-F. Zhao, A.-T. Le, C. Jin, X. Wang, and C. D. Lin, *Phys. Rev. A* **93**, 023413 (2016).
- [24] Y. H. Lai, J. Xu, U. B. Szafruga, B. K. Talbert, X. Gong, K. Zhang, H. Fuest, M. F. Kling, C. I. Blaga, P. Agostini, and L. F. DiMauro, *Phys. Rev. A* **96**, 063417 (2017).
- [25] Z. Chen, A.-T. Le, T. Morishita, and C. D. Lin, *Phys. Rev. A* **79**, 033409 (2009).
- [26] C. D. Lin, A.-T. Le, C. Jin, and H. Wei, *Attosecond and Strong-Field Physics Principles and Applications* (Cambridge University Press, Cambridge, UK, 2018).
- [27] C. D. Lin, A.-T. Le, C. Jin, and H. We, *J. Phys. B: At., Mol. Opt. Phys.* **51**, 104001 (2018).
- [28] M. Y. Kuchiev, *J. Phys. B: At., Mol. Opt. Phys.* **28**, 5093 (1995).
- [29] E. Clementi and C. Roetti, *At. Data Nucl. Data Tables* **14**, 177 (1974).
- [30] O. Zatsarinny and K. Bartschat, *J. Phys. B: At., Mol. Opt. Phys.* **46**, 112001 (2013).
- [31] T. Morishita, Z. Chen, S. Watanabe, and C. D. Lin, *Phys. Rev. A* **75**, 023407 (2007).
- [32] B. Feuerstein, R. Moshhammer, D. Fischer, A. Dorn, C. D. Schröter, J. Deipenwisch, J. R. Crespo Lopez-Urrutia, C. Höhr, P. Neumayer, J. Ullrich, H. Rottke, C. Trump, M. Wittmann, G. Korn, and W. Sandner, *Phys. Rev. Lett.* **87**, 043003 (2001).
- [33] G. L. Yudin and M. Yu. Ivanov, *Phys. Rev. A* **63**, 033404 (2001).
- [34] N. Ekanayake, Sui Luo, B. L. Wen, L. E. Howard, S. J. Wells, M. Videtto, C. Mancuso, T. Stanev, Z. Condon, S. LeMar, A. D. Camilo, R. Toth, W. B. Crosby, P. D. Grugan, M. F. Decamp, and B. C. Walker, *Phys. Rev. A* **86**, 043402 (2012).
- [35] R. Moshhammer, B. Feuerstein, W. Schmitt, A. Dorn, C. D. Schröter, J. Ullrich, H. Rottke, C. Trump, M. Wittmann, G. Korn, K. Hoffmann, and W. Sandner, *Phys. Rev. Lett.* **84**, 447 (2000).
- [36] W. Lotz, *Z. Phys.* **216**, 241 (1968).
- [37] X. M. Tong, Z. X. Zhao, and C. D. Lin, *Phys. Rev. A* **68**, 043412 (2003).
- [38] A. Becker and F. H. M. Faisal, *Phys. Rev. A* **59**, R3182 (1999).
- [39] S. Palaniyappan, A. DiChiara, E. Chowdhury, A. Falkowski, G. Ongadi, E. L. Huskins, and B. C. Walker, *Phys. Rev. Lett.* **94**, 243003 (2005).
- [40] S. Micheau, Z. Chen, A.-T. Le, and C. D. Lin, *Phys. Rev. A* **79**, 013417 (2009).
- [41] S. Larochelle, A. Talebpoury, and S. L. Chin, *J. Phys. B: At., Mol. Opt. Phys.* **31**, 1201 (1998).
- [42] P. J. Ho and J. H. Eberly, *Phys. Rev. Lett.* **95**, 193002 (2005).
- [43] T. Brabec, M. Yu. Ivanov, and P. B. Corkum, *Phys. Rev. A* **54**, R2551 (1996).